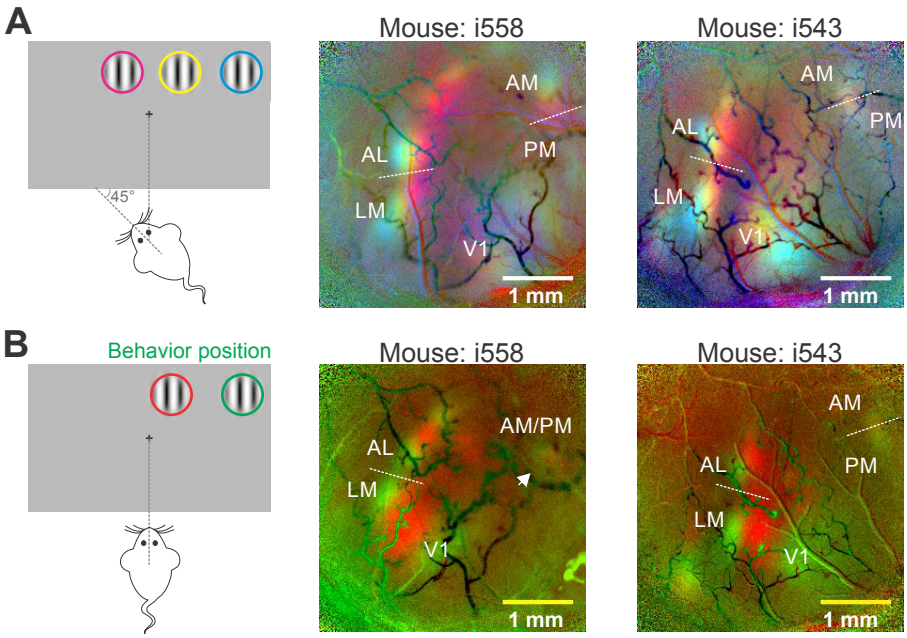

Figure S1. Identification of boundaries between visual cortical areas using intrinsic autofluorescence imaging. Related to Figure 1. (**A**) Change in intrinsic autofluorescence for two example mice (right) in response to visual stimuli presented at three positions (left) when animal is rotated 45° relative to the screen. Colors in the map match the positions outlined in the schematic (azimuth -10°, 10° and 30°, elevation of 10°). Lines show identified boundaries between AL and LM, AM and PM. (**B**) Same as **A**, for responses to the two positions (azimuth 10-20° and 30-40°, elevation 10°) when the same animals are perpendicular to the monitor. Arrowhead points to the place where AM and PM were not entirely separable at the behavior position (green). Note that mouse i558 is the same mouse in **Figure 1A**.

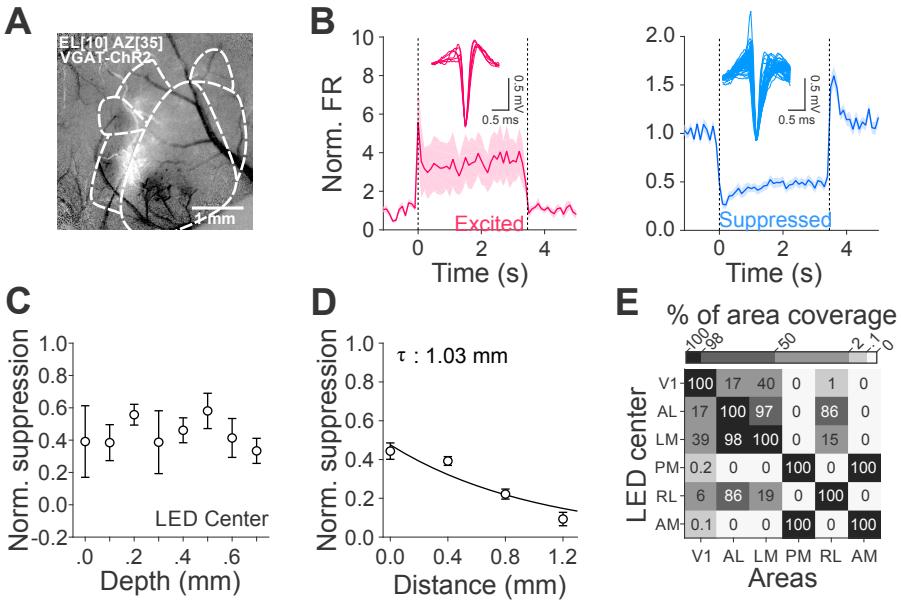

Figure S2. Efficacy and spatial resolution of optogenetic inhibition in VGAT-ChR2 transgenic mouse line. Related to Figure 1. (**A**) Cortical reflectance in response to a visual stimulus at elevation 10°, azimuth 35°, size 40°. Decreases in reflectance reflect activation. (**B**) Normalized spontaneous firing rates (FR) of cells that are excited (left, red, n=6 cells) and suppressed (right, blue, n=42 cells) when stimulated with 450 nm laser. Dashed lines indicate laser onset and offset. Insets are the waveforms of single units. Light power: 0.4-0.5 mW across 9 experiments (n=2 mice). (**C**) Normalized suppression as a function of cortical depth in the laser center. Error bars are SEM across cells (n=5, 3, 5, 6, 11, 8, 7, 8 cells, from superficial to deep). (**D**) Normalized suppression as a function of distance from the laser center (0 mm). Error bars are SEM across cells (n=53, 125, 64, 20, from 0 to 1.2 mm). The decay constant (τ) was calculated via a single exponential fit. (**E**) Mean percentage of area coverage of inhibition across mice (n=15)**.**

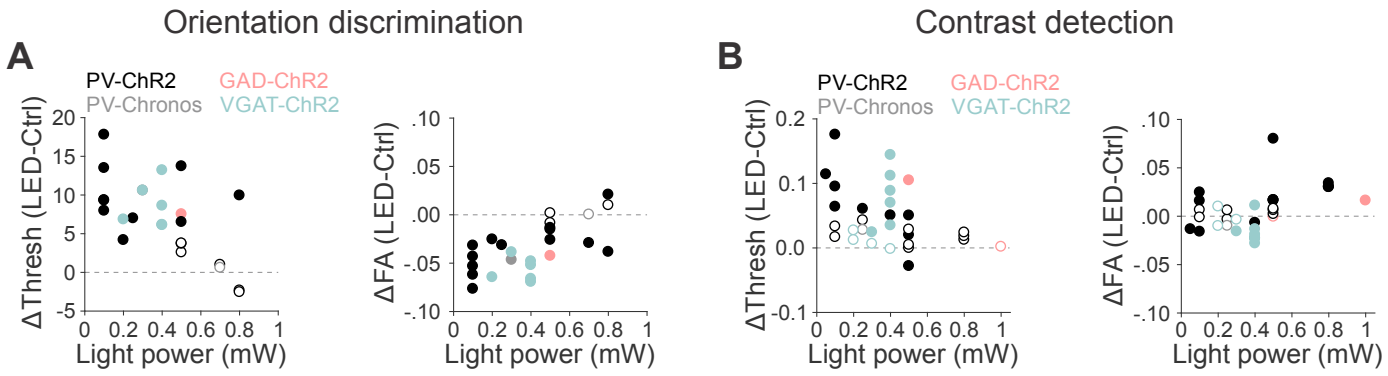

Figure S3. Effects of suppression method and light power on behavior performance in orientation discrimination and contrast detection tasks. Related to Figures 2 and 4. (**A**) Effects of area suppression on orientation discrimination threshold (left) and FA rate (right) as a function of light power. Different colors denote different suppression methods. Filled and open circles denote significant and non-significant difference between control and suppression trials. (**B**) Same as **A**, for the performance in the contrast detection task.

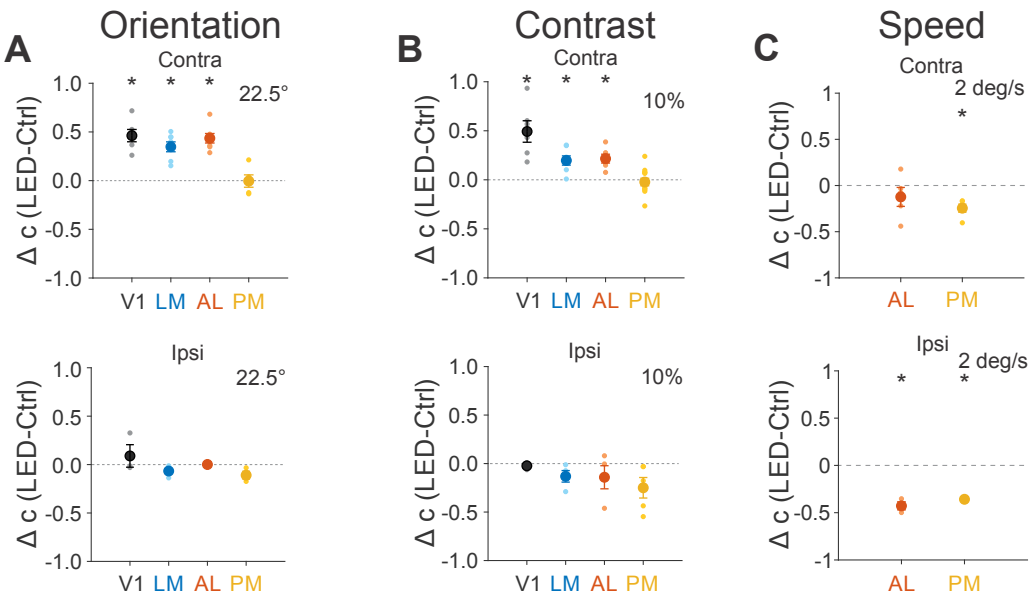

Figure S4. Effects of area suppression on bias measure for three visual tasks. Related to Figures 2, 4 and 5. (**A**) Summary of change in bias (c) when suppressing contralateral (contra, top) and ipsilateral (ipsi, bottom) areas during the orientation discrimination task. (**B-C**) Same as **A**, for contrast detection (**B**) and speed increment detection (**C**) tasks. * p<0.05.

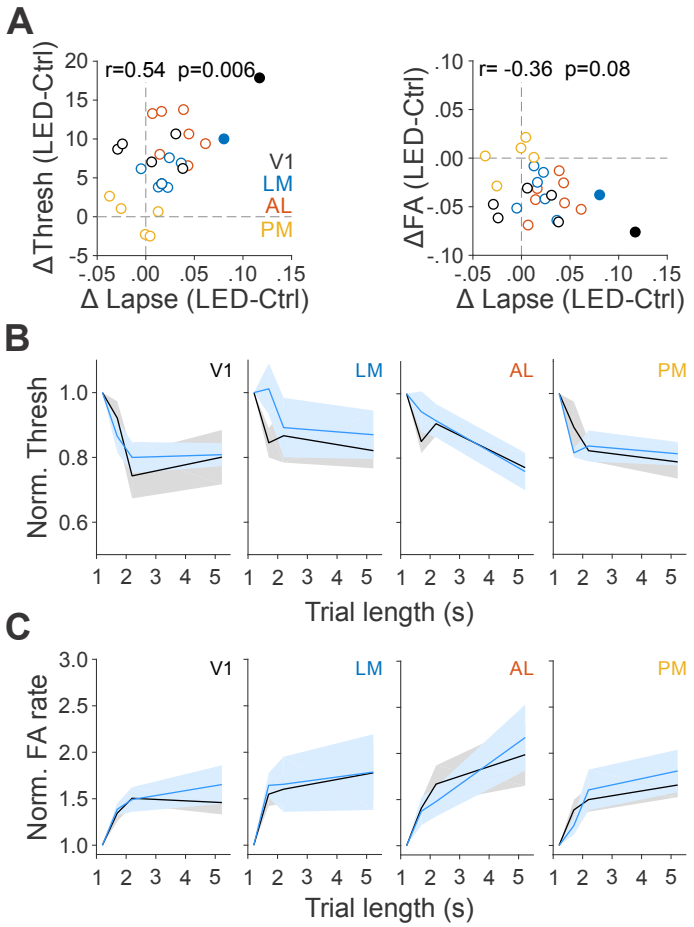

Figure S5. Lack of effects of area suppression on engagement and expectation. Related to Figure 2. (**A**) Changes in orientation discrimination threshold (left) and FA rate (right) plotted against changes in lapse rate. Different colors denote different visual areas. Filled and open circles denote significant and non-significant difference in lapse rate between control and suppression trials. (**B**) Summary of normalized orientation discrimination threshold over trial length bins (950-1450, 1450-1950, 1950-2450, 2450-8000 ms) for control (black) and suppression (blue) trials. Shaded areas are SEM across mice (n=5, 4, 5, 5 for V1, LM, AL, and PM respectively). (**C**) Same as (**B**) for FA rate.